Heliyon 10 (2024) e33302

Contents lists available at ScienceDirect

Heliyon

journal homepage: www.cell.com/heliyon

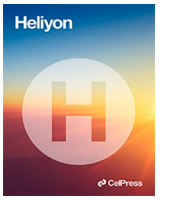

Research article

Gold nanoparticles coated with collagen-I and their wound healing activity in human skin fibroblast cells

Sasiprapa Poomrattanangoon [a,b], Dakrong Pissuwan [a,b,*]

[a] Materials Science and Engineering Program, Faculty of Science, Mahidol University, Bangkok 10400, Thailand
[b] Nanobiotechnology and Nanobiomaterials Research Laboratory, School of Materials Science and Innovation, Faculty of Science, Mahidol University, Bangkok 10400, Thailand

ARTICLE INFO

Keywords:
Gold nanoparticles
Collagen
Skin fibroblast cells
Wound healing
Inflammatory cytokine

ABSTRACT

The slow wound healing process has become a major health problem. Gold nanoparticles (AuNPs) have been used in various biomedical applications because of their unique properties. Type I collagen (Collagen-I) is a protein and be the most abundant type of collagen. This type of collagen can help the surrounding structure to maintain its rigidity. In this study, we stabilized the surface of AuNPs using Collagen-I (Collagen-I@AuNPs) and investigated the effect of Collagen-I@AuNPs on wound healing. The evaluation of inflammatory cytokine secretion, which were interleukin-6 (IL-6) and tumour necrosis factor-alpha (TNF-α), was performed. We found that Collagen-I@AuNPs reduced the levels of IL-6 and TNF-α in scratched human skin fibroblast (HSF) cells. Furthermore, Collagen-I@AuNPs induced the expression of basic fibroblast growth factor (bFGF) and vascular endothelial growth factor (VEGF), which are key growth factors involved in wound healing. This results in enhanced wound closure. In addition, Collagen-I@AuNPs were not toxic to HSF cells and facilitated the cellular uptake of particles inside HSF cells. Therefore, Collagen-I@AuNPs is a promising candidate for wound healing enhancement.

1. Introduction

It is well-known that the skin acts as the first barrier to protect the body from chemicals, microorganisms, and other substances. Therefore, when skin is damaged, it is important to heal the damaged skin over a short period. Skin healing is a natural mechanism that protects the human body and involves complex biological processes related to cell inflammation, proliferation, and remodeling. Various cell types, growth factors, and extracellular matrix function together during the wound healing process [1]. Slow wound healing can cause infections and complicated tissue defects [2]. In particular, chronic wounds infected with pathogenic bacteria can lead to difficult wound malmanagement [3]. Currently, many treatments are used to treat wounds and enhance wound healing processes, including wound dressing, hyperbaric oxygen therapy, and negative pressure wound therapy [4]. However, these methods have limitations resulting in ineffective wound repair. Therefore, a novel approach is required to accelerate the wound-healing process. It has been reported that wound healing process requires adequate nutrients including amino acids [5,6]. Collagen plays a vital role in the wound healing. This is because collagen is involved in molecular biomechanics such as elasticity, tensile strength, and structural stability of body tissues [7]. When an injury occurs, collagen induces the activation and aggregation of pellets, leading to the

* Corresponding author. Nanobiotechnology and Nanobiomaterials Research Laboratory, School of Materials Science and Innovation, Faculty of Science, Mahidol University, Bangkok 10400, Thailand.
E-mail address: dakrong.pis@mahidol.ac.th (D. Pissuwan).

https://doi.org/10.1016/j.heliyon.2024.e33302
Received 17 January 2024; Received in revised form 16 May 2024; Accepted 18 June 2024
Available online 20 June 2024

formation of fibrin clots at the injury site. Collagen aids in the recruitment of fibroblasts, epithelial, and endothelial cells during inflammation and facilitates tissue remodeling and tensile strength development [8]. Furthermore, collagen can be found in the scar tissue that forms during the process of wound healing [9]. Owing to the vital role of collagen in the wound healing process, interest in the application of collagen for wound treatment has increased. There are 29 known types of collagen [3]. Type I collagen (Collagen-I) is the most abundant and found in various mammalian connective tissues. In the skin, there is approximately 70 % Collagen-I and 10 % type III collagen. Collagen-I is mainly present in the dermal extracellular matrix (ECM) and plays a key role in wound repair [10]. This type of collagen can also enhance cell proliferation [11].

Nanomaterials have attracted growing interest in recent years. They are small and can easily penetrate into cells. Gold nanoparticles (AuNPs) are metal nanoparticles with excellent biological properties [12]. The biocompatibility of AuNPs can be managed by regulating their sizes, surface properties, and dosages [13]. Therefore, AuNPs are of interest for various biomedical applications [14], such as photothermal therapy [15], drug and gene delivery [16], diagnosis [17,18], and regenerative medicine [19]. Based on recent studies, it appears that AuNPs can facilitate the healing process [20,21]. It has been reported that AuNPs can induce wound healing by engaging in anti-inflammatory and anti-angiogenic activities, such as inducing vascular endothelial growth factor (VEGF) expression [22] and potentially functioning as antioxidants [23]. Furthermore, AuNPs can increase collagen expression, which can enhance cutaneous wound healing [24]. The surface of AuNPs can be easily modified; therefore, numerous studies have demonstrated the potential of AuNP surface modification using active biological molecules to promote wound healing. For example, spherical AuNPs coated with peptides have been developed to modulate angiogenesis, which is a process involving blood vessel formation [25]. This blood vessel formation also plays an important role in the healing process of wounds [26]. AuNPs were coated with two different outer layers, chitosan and poly-L-arginine, indicating the efficiency of these formulations in increasing the levels of pro-angiogenic factors such as vascular endothelial growth factor (VEGF) and fibroblast growth factor 2 (FGF-2). Angiogenic growth factors can improve the healing of wounds by promoting the growth of new blood vessels. Li et al. [27,72–76] conjugated keratinocyte growth factor (KGF) with AuNPs and found that this conjugation could accelerate wound recovery in diabetic rats. In addition, collagen/AuNP nanocomposites were found to be a promising material for skin wound healing due to their biocompatibility and ability to effectively stimulate wound healing [28]. The combination of AuNPs and collagen as new materials for biomedical applications was also demonstrated by Castaneda et al. [29]. They demonstrated that the use of their prepared AuNPs at a low concentration in the crosslinking of collagen gels did not produce toxic effect to 3T3 fibroblasts. According to the report of Xing et al. [30], a colloidal gold−collagen protein core−shell nanoconjugate has been demonstrated to promote cellular activities such as cell adhesion, cell growth, and cell differentiation.

Based on the benefits of collagen and AuNPs and the existing literature, in this work, we aimed to explore the potential effect of AuNPs coated with Collagen-I (Collagen-I@AuNPs) on the wound healing process because of the limited available information regarding this specific type of conjugation. Human skin fibroblasts were used as model cells for the *in vitro* wound healing study. The effects of Collagen-I@AuNPs on wound closure, cell proliferation, pro-inflammatory responses, and growth factor generation were investigated in this study.

2. Material and methods

2.1. Materials

Hydrogen tetrachloroaurate (III) trihydrate ($HAuCl_4 \cdot 3H_2O$, 99.9 %) and trisodium citrate dihydrate ($Na_3C_6H_5O_7 \cdot 2H_2O$) were purchased from Sigma-Aldrich (St. Louis, MO, USA). Rat tail collagen at a concentration of 2 mg mL^{-1} was purchased from Serva (Heidelberg, Germany). Dulbecco's Modified Eagle Medium (DMEM) high glucose medium, fetal bovine serum (FBS), and 1 % penicillin/streptomycin were purchased from HIMEDIA (Mumbai, India). CellTiter-Glo luminescent cell viability assay and CellTiter 96 AQueous one solution cell proliferation assay were purchased from Promega (Madison, USA). Phosphate buffer saline (PBS) with Ca^{2+} and Mg^{2+} solution (100x) and Roswell Park Memorial Institute (RPMI) 1640 were purchased from NacalaiTesque (Kyoto, Japan). ELISA MAX Deluxe Set Human IL-6, fibroblast growth factor (bFGF), and TNF-alpha were purchased from Biolegend (San Diego, United States of America). The Human VEGF ELISA kit was purchased from Abcam (Cambridge, United States of America).

2.2. Synthesis of AuNPs

AuNPs were synthesized via a citrate reduction reaction using the Turkevich method [31]. First, a 5 mL solution of $HAuCl_4$ was diluted in 45 mL of Milli-Q water and stirred with a magnetic stirrer. Heat was applied until the temperature reached 95 °C. Then, trisodium citrate dihydrate at 19.4 mM was added to the $HAuCl_4$ solution while stirring at a high speed. When the solution turned ruby red, it was continuously stirred under heat for 15 min. Afterward, the solution was stirred without heating for another 15 min. Finally, the spherical AuNPs were stored at 4 °C for future experiments.

2.3. Conjugation of AuNPs with collagen

The optical density (O.D.) of AuNPs at a wavelength of 522 nm was adjusted to 1.0 and the pH was adjusted to 7.0 using 0.5 M NaOH. Subsequently, spherical AuNPs ($O.D._{522\ nm} = 1.0$), rat tail Collagen-I (2 mg mL^{-1}), and Milli-Q water were mixed at a ratio of 3:2:1, respectively. The solution was then mixed using a shaker at room temperature for 15 min. Following this process, the solution was centrifuged 3 times at 9,391 × *g* for 10 min at room temperature and the pellet of Collagen-I@AuNPs conjugates was re-dispersed

with Milli-Q water. The Collagen-I@AuNPs conjugates were further examined using a UV–vis spectrophotometer to measure their absorbance.

2.4. Characterization of AuNPs and Collagen-I@AuNPs

The light absorptions of the AuNPs and Collagen-I@AuNPs were measured using a UV–vis spectrophotometer (UV-2550, Shimadzu, Japan). The morphologies of AuNPs and Collagen-I@AuNPs were investigated by transmission electron microscopy (TEM) [32]. The samples were stained with 2 % uranyl acetate dissolved in Milli-Q water before TEM observation. Zeta potential and polydispersity index (PDI) were measured using dynamic light scattering (DLS, Malvern, UK). Infrared (IR) spectra were obtained using a Fourier transform IR spectrometer (PerkinElmer, USA).

2.5. Cell culture

Human skin fibroblast (HSF) cells, from the National Institute of Biomedical Innovation, Health and Nutrition (NIBIOHN), were cultured in DMEM, high glucose medium supplemented with 10 % FBS and 1 % penicillin/streptomycin. The HSF cells were maintained at 37 °C in a 5 % CO_2 incubator.

2.6. Cell viability

HSF cells at a concentration of 1×10^4 cells per well were cultured in 96-well plates and incubated for 24 h at 37 °C in a 5 % CO_2 incubator. The culture medium (high glucose DMEM with 10 % FBS and 1 % penicillin/streptomycin) was then removed and 200 μL of medium containing different concentrations of AuNPs or Collagen-I@AuNPs (0, 3, 5, 10, 15, and 25 μg mL^{-1}) was added and incubated for 24 h. Cells without AuNPs or Collagen-I@AuNPs were cultured in the same medium (200 μL) as the control group. After 24 h, the viability of cells treated with AuNPs with or without collagen coating was determined using the CellTiter-Glo luminescent cell viability assay kit (Promega, Madison, WI, United States of America). The protocol provided by the manufacturer of the cell viability assay kit was used during the testing process. Briefly, the treated HSF cells were washed twice with PBS containing Ca^{2+} and Mg^{2+}. Following this, RPMI 1640 (100 μL) was added to the cell sample, followed by the CellTiter-Glo solution (100 μL). The cell samples were shaken gently for 10 min in the absence of light. Thereafter, luminescent signals were measured using a microplate reader (TECAN Spark 10 M, Männedorf, Switzerland).

2.7. Cell proliferation

HSF cells at a concentration of 1×10^4 cells per well were cultured in 96-well plates and incubated for 24 h at 37 °C in a 5 % CO_2 incubator. The same type and amount of medium containing different concentrations of AuNPs and Collagen-I@AuNPs, as mentioned in the cell viability assay, were applied to HSF cells and incubated for 24 h. This incubation time was selected to investigate the effect of AuNPs and Collagen-I@AuNPs on the induction of cell proliferation at an early time point. After incubation, a CellTiter 96 AQueous one solution cell proliferation assay kit (Promega, Madison, WI, United States of America) was used to measure cell proliferation using the protocol provided by the commercial kit. Briefly, cell samples were washed twice with PBS containing Ca^{2+} and Mg^{2+}. Thereafter, 100 μL of RPMI 1640 and 20 μL of CellTiter 96 AQueous one solution were added to the cell samples. The cell samples were then incubated at 37 °C in a 5 % CO_2 incubator for 4 h. Finally, the absorbance of the mixture was measured at 490 nm wavelength using a microplate reader (TECAN Spark 10 M, Männedorf, Switzerland).

2.8. Wound scratch assay

HSF cells at a concentration of 5.7×10^4 cells per well were cultured in 24-well plates and incubated for 24 h. The high glucose DMEM containing 10%FBS and 1 % penicillin/streptomycin was used for cell culture. The HSF cells were then scratched with a sterile 10 mL plastic pipette. The cells were washed with PBS containing Ca^{2+} and Mg^{2+}. Following this, AuNPs and Collagen-I@AuNPs (3 μg mL^{-1}) were added. The high glucose DMEM medium supplemented with 5 % FBS and 1 % penicillin/streptomycin was used in this experiment. The cells were incubated for 24, 48, and 72 h. Control cells were cultured in media without nanoparticles. The area of cell migration was measured using the ImageJ software.

2.9. Cellular uptake of AuNPs and Collagen-I@AuNPs

The amounts of AuNPs and Collagen-I@AuNPs taken up by HSF cells were investigated using inductively coupled plasma mass spectrometry (ICP-MS). HSF cells at a concentration of 5.7×10^4 cells per well were cultured in 24-well plates for 24 h, after which they were scratched using the same approach as that used for the wound scratch assay. The high glucose DMEM medium containing 10 % FBS and 1 % penicillin/streptomycin was used. Next, the scratched HSF cells were treated with 3 μg mL^{-1} AuNPs and Collagen-I@AuNPs for 24, 48, and 72 h. Following treatment, the scratched HSF cells were lysed with 250 μL lysis buffer and sonicated for 30 min to damage the cell membrane. The cells were then incubated in digested buffer (3 mL of 65 % HCl and 1 mL of 6 % H_2O_2) overnight in a chemical fume hood. After incubation, the aqua regia (3:1 ratio of HCl to HNO_3) at a volume of 3 mL was added to the cells and incubated for another 2 h [33]. After completely cell digestion, the digested cells were diluted with Milli-Q water to obtain a

final concentration of 5 % aqua regia in the total volume of cell suspension. Standard gold chloride solutions were prepared at concentrations of 0, 2.5, 5, 10, 15, 25, and 50 μg L^{-1}. The gold content in the cell samples was determined using ICP-MS (Agilent Technologies, Santa Clara, CA, United States of America).

2.10. Enzyme-linked immunosorbent assay

To investigate the production of inflammatory cytokines (interleukin-6 (IL-6)), tumor necrosis factor-α (TNF-α) and angiogenic growth factors (vascular endothelial growth factor (VEGF) and basic fibroblast growth factor (bFGF)), ELISA kits from Biolegend and Abcam were employed. The supernatant from the wound scratch assay was gathered and preserved at −80 °C for ELISA analysis, following the manufacturer's instruction. The signals were observed at 450 nm using a microplate reader (Azure Biosystem, Dublin, CA, United States of America).

2.11. Attenuated total reflectance (ATR)-FTIR analysis

The solution of AuNPs or Collagen-I@AuNPs at a volume of 1 mL was centrifuged at 9, 319×*g* at room temperature for 10 min to obtain the pellet. Following this, the pellet was dropped on a glass slide and left to dry in a silica gel box. Thereafter, a high concentration of samples was prepared by repeatedly dropping the pellet onto a glass slide 10 times. The prepared samples were ready for ATR-FTIR (PerkinElmer, Waltham, MA, United States of America) measurements in the range of 4000 to 400 cm^{-1} at a spectral resolution of 4 cm^{-1}. Sixteen scans were conducted per sample.

2.12. Statistical analysis

All experimental data are presented as mean ± standard error. Statistical analyses were performed using the GraphPad Prism software version 8.0. ANOVA and Tukey-Kramer tests were used to determine statistical significance at $P \leq 0.05$.

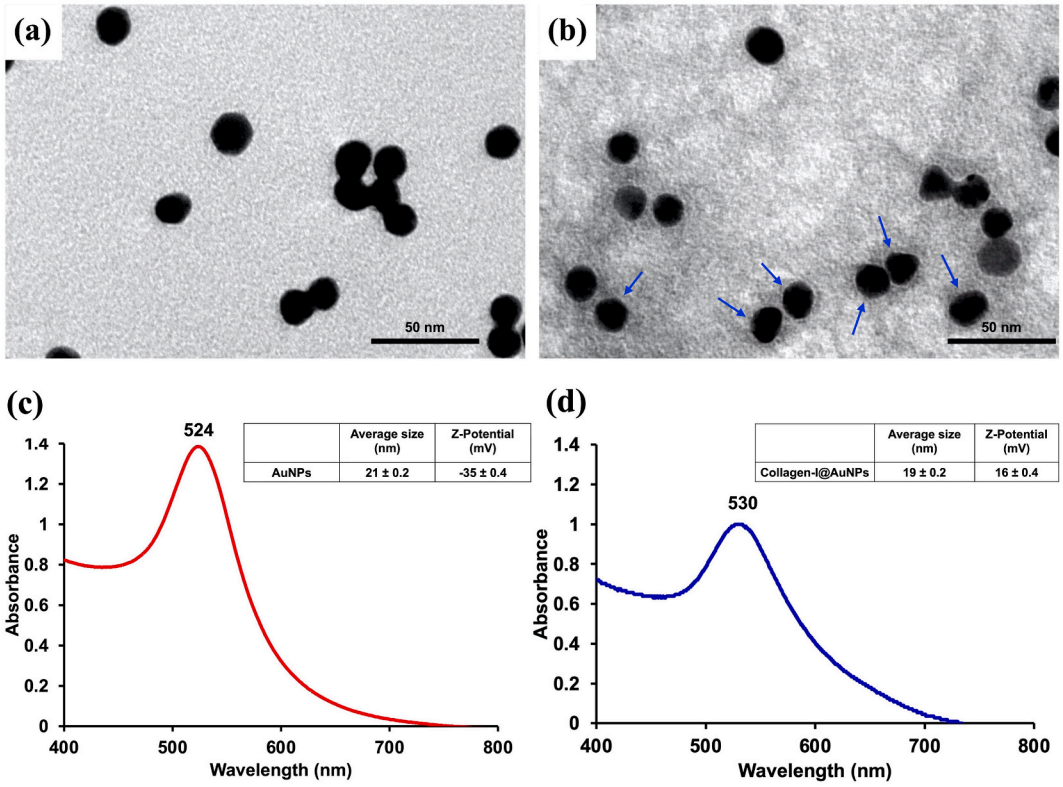

Fig. 1. TEM images of (a) AuNPs and (b) Collagen-I@AuNPs (arrows indicates dark staining of Collagen-I) and light absorption spectra of (c) AuNPs and (d) Collagen-I@AuNPs.

3. Results and discussion

3.1. Characterization of AuNPs and Collagen-I@AuNPs

The morphology of AuNPs was spherical (Fig. 1a) with an average size of ~21 ± 0.2 nm. As expected, Collagen-I@AuNPs (Fig. 1b) were spherical with an average size of ~19 ± 0.2 nm. After staining the samples with uranyl acetate, the dark staining of Collagen-I was detected on the surface of AuNPs (Fig. 1b). This indicates an interaction between Collagen-I and AuNPs. In contrast, unconjugated AuNPs did not show any dark staining. The peak of the maximum light absorption for AuNPs was observed at ~524 nm (Fig. 1c), but a redshift in the absorption spectrum was observed for the Collagen-I@AuNPs. As shown in Fig. 1d, the maximum light absorption peak of the Collagen-I@AuNPs was at ~530 nm. An average zeta potential value of AuNPs was found to be negative (−35 ± 0.4 mV). In contrast, Collagen-I@AuNPs exhibited an average positive zeta potential value of 16 ± 0.4 mV. The reported positive zeta potential of metal nanomaterials stabilized with Collagen-I is also noteworthy by Cardoso et al. [34]. An increase in zeta potential value from −35 ± 0.4 mV to 16 ± 0.4 mV indicates that the surface of AuNPs was successfully modified by collagen.

We additionally examined the stability of Collagen-I@AuNPs (refer to supplementary material section; Fig. S1&S2) and found that the stability of Collagen-I@AuNPs exhibited a slight change following storage in a suspension (dispersed in Milli-Q water) for a week at 4 °C. Similarly, the dispersion of Collagen-I@AuNPs in culture media containing 10 % FBS produced comparable results after one-week storage. However, the storage of Collagen-I@AuNPs in pellet form maintained good stability after a week of storage and then dispersed in aqueous media, such as Milli-Q water or cell culture media. Although we did not investigate the maximum time that Collagen-I@AuNPs can be stored in this study, based on the available data, it appears that long-term storage is possible and the storage of Collagen-I@AuNPs in the form of conjugated pellets was more advantageous in terms of stability than the suspension.

Furthermore, ATR-FTIR analysis was performed to investigate conformational changes of collagen or AuNPs after their interaction. As seen in Fig. 2, the ATR-FTIR spectrum of AuNPs exhibited the strong peaks at ~2915 cm^{-1} (ν-stretching vibration of C–H; ν(C–H)), 2848 cm^{-1} (ν(C–H), 1561 cm^{-1} (ν_{asy}-asymmetric stretching vibration of COO^-; $\nu_{asy}(COO^-)$), 1386 cm^{-1} ($\nu(COO^-)$), and 1078 cm^{-1}(asymmetric stretching vibration of the alcohol group; $\nu_{asy}(C–O)_{alch}$) [35]. The ATR-FTIR spectrum of typeI collagen was also measured. The spectrum vibration peak of collagen at ~3283 cm^{-1} indicates the band of amide A owing to the vibration of N–H stretching (ν(N–H)) [36]. The next peak at 2928 cm^{-1} corresponds to the amide B band from $\nu_{asy}(CH_2)$) [37]. The amide I band was also detected at the peak of ~1633 cm^{-1} due to the stretching vibration of the peptide carbonyl group (-C═O) of the polypeptide backbone [38]. The peak at ~1544 cm^{-1} corresponds to amide II arising from the N–H bending vibration and C–N stretching [39]. Additionally, the amide III was also detected through the peak at ~1238 cm^{-1} originating from the vibrations of H-bonds [40]. In the case of Collagen-I@AuNPs, a small shift in the peak position of Collagen-I peak was observed at ~3289 cm^{-1}. Changes in other peaks were also detected such as the peak at ~2915 cm^{-1}, which could indicate the interaction between AuNPs and Collagen-I. The peak detected for Collagen-I, at ~1544 cm^{-1}, was also detected in Collagen-I@AuNPs at ~1543 cm^{-1}. Many peaks detected in the AuNPs changed their positions after interacting with Collagen-I. Therefore, the ATR-FTIR results strongly confirmed the change in the original structure of Collagen-I and AuNPs due to the interaction between Collagen-I and AuNPs.

3.2. Cell viability and cell proliferation of HSF cells treated with AuNPs and Collagen-I@AuNPs

In this section, the effect of AuNPs and Collagen-I@AuNPs on the cell viability of HSF cells was investigated. AuNPs and Collagen-I@AuNPs at different concentrations (3, 5, 10, 15, and 25 μg mL^{-1}) were applied to HSF cells for 24 h and cell viability was measured.

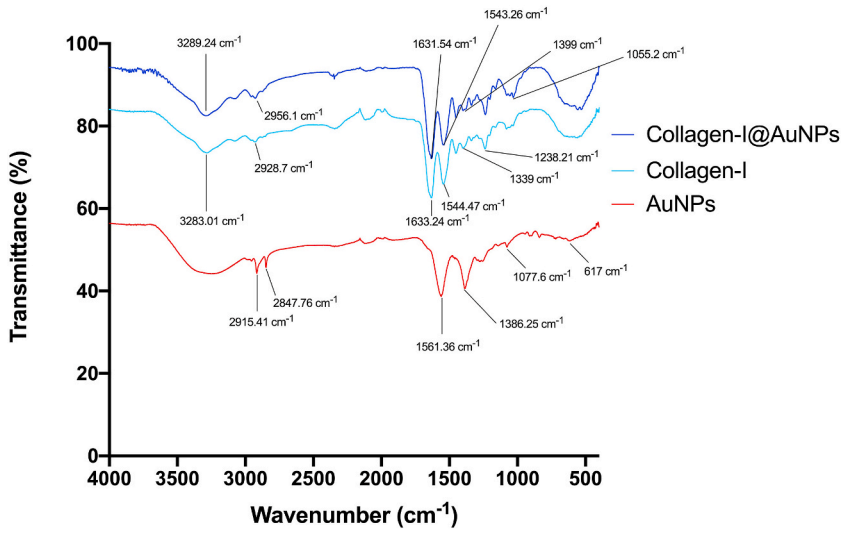

Fig. 2. FTIR spectra of AuNPs, collagen-I, and Collagen-I@AuNPs.

As shown in Fig. 3 (a&b), the relative cell viability of HSF cells treated with AuNPs and Collagen-I@AuNPs was higher than 95 % at all treatment concentrations. When HSF cells were treated with Collagen-I@AuNPs, the cell viability of HSF cells was slightly higher than that of cells treated with AuNPs. The cell viability of HSF cells after treating with 3, 5, 10, 15, and 25 μg mL^{-1} Collagen-I@AuNPs were 100.38 ± 3.51 %, 101.87 ± 2.40 %, 101.43 ± 2.32 %, 97.18 ± 2.25 %, and 97.40 ± 1.18 % respectively. According to Cardoso et al. [34], the use of Collagen-I to stabilize metal nanoparticles did not result in the induction of early and late apoptosis, and necrosis in fibroblast cells. Compared to control cells, a significant reduction in cell viability was found in HSF cells treated with AuNPs at concentrations of 15 and 25 μg mL^{-1} (95.08 ± 0.68 % and 96.18 ± 0.56 %, respectively). According to ISO 10993-5, these percentages of cell viability (>80 %) can be considered non-cytotoxic [41]. Therefore, AuNPs and Collagen-I@AuNPs used in this study were considered to be non-cytotoxic.

Cell proliferation was determined to obtain more information on the metabolic function of HSF cells after treatment with AuNPs and Collagen-I@AuNPs. We found that AuNPs did not significantly affect cell proliferation. The relative proliferation percentage of HSF cells did not decrease significantly after treatment with AuNPs (Fig. 4a). The proliferation of HSF cells was found to be significantly induced when treated with Collagen-I@AuNPs at concentrations ranging from 3 to 25 μg mL^{-1} (Fig. 4b). The percentages of relative cell proliferation ~135 % were detected in HSF cells treated with Collagen-I@AuNPs at concentrations of 3 μg mL^{-1} (135.21 ± 6.69 %) and 5 μg mL^{-1} (135.42 ± 7.7.6 %). A higher percentage of cell proliferation was found in cells treated with 10 μg mL^{-1} (151.15 ± 9.07 %), 15 μg mL^{-1} (154.59 ± 4.70 %), and 25 μg mL^{-1} (154.74 ± 9.72 %) (Fig. 4b). The outcome of these findings reveals that the coating of Collagen- I coating on the surface of AuNPs can substantially promote HSF cell proliferation. This could be because Collagen-I is a vital protein in skin fibroblasts [42]; therefore, it strongly enhances cell proliferation.

3.3. Cellular uptake of AuNPs and Collagen-I@AuNPs by scratched HSF cells

Cellular uptake of AuNPs and Collagen-I@AuNPs was quantitatively evaluated using ICP-MS. This technique can be used to determine the concentration of Au atoms based on the cellular uptake of AuNPs or Collagen-I@AuNPs. In this cellular uptake investigation, AuNPs and Collagen-I@AuNPs at a concentration of 3 μg mL^{-1}were used because the cells were healthy at this concentration after treatment. Scratched HSF cells were treated with 3 μg mL^{-1} AuNPs and Collagen-I@AuNPs at different time points from 24 to 72 h. After culturing scratched HSF cells with 3 μg mL^{-1}AuNPs for 24 h and 48 h, AuNPs were not detected. This indicates that AuNPs were failed to be internalized by scratched HSF cells. A small amount of gold at ~0.25 ± 0.01 μg L^{-1} was found in scratched HSF cells cultured with 3 μg mL^{-1}AuNPs for 72 h (Fig. 5a). These data indicate that the incubation time affected the cellular uptake of AuNPs. An increase in the Au mass detected in cells after increasing incubation time was also reported by Wang et al. [43]. It is important to note that cellular uptake in this study was investigated in scratched HSF cells, but not in healthy cells. To the best of our knowledge, our research is the first to investigate the cellular uptake of AuNPs in scratched HSF cells. The function of cells to absorb substances may be negatively impacted by cell injury.

In the case of scratched HSF cells treated with 3 μg mL^{-1} Collagen-I@AuNPs for 72 h, the gold content detected in scratched HSF cells was ~7.56 ± 0.26 μg L^{-1}. At 24 and 48 h of treatment, the gold contents detected in scratched HSF cells were 6.09 ± 0.26 μg L^{-1} and 6.66 ± 0.77 μg L^{-1} respectively (Fig. 5a). Our results clearly demonstrated that Collagen-I@AuNPs had a higher degree of internalization than AuNPs. A study by Marisca et al. [44] also demonstrated that cellular uptake of AuNPs coated with collagen were highly uptake by cells. Additionally, the highest level of internalization of collagen coated on nanoparticles was observed, when compared with other protein coatings [45]. This indicates that Collagen-I can enhance the adhesion of particles to cells, resulting in the

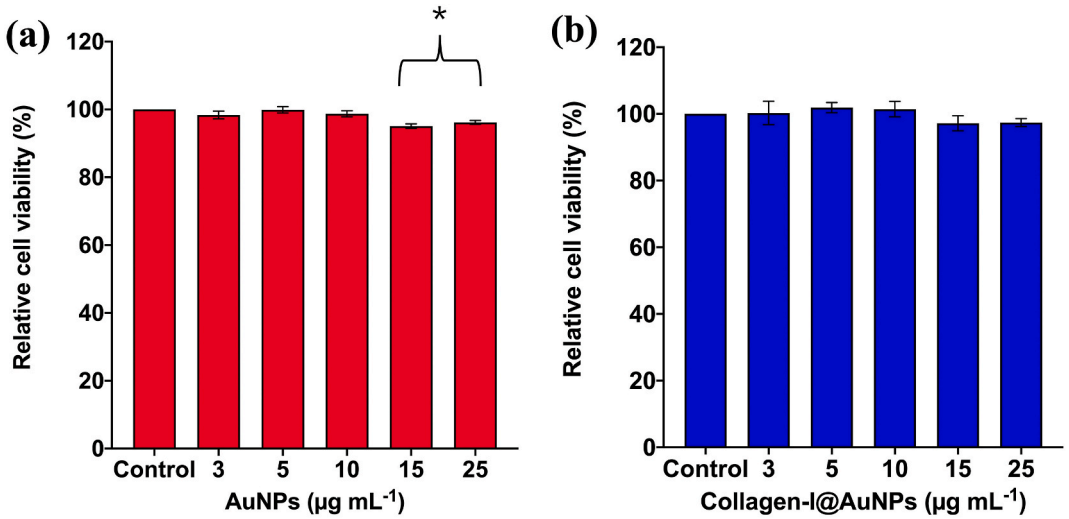

Fig. 3. Relative cell viability of HSF cells treated with (a) AuNPs and (b) Collagen-I@AuNPs. An asterisk indicates a significant difference in cell viability compared with untreated HSF cells (control; $P < 0.05$). Statistical analysis was performed using Turkey-Kramer ($n \geq 7$).

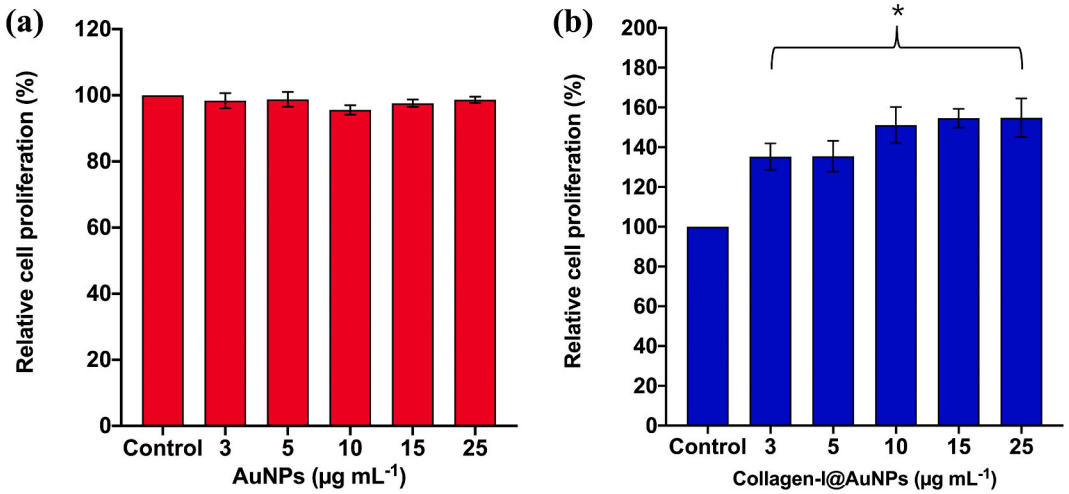

Fig. 4. Cell proliferation of (a) AuNPs and (b) Collagen-I@AuNPs. An asterisk indicates a significant difference in cell proliferation at $P < 0.05$ compared with untreated HSF cells (control). Statistical analysis was performed by Turkey-Kramer ($n \geq 3$).

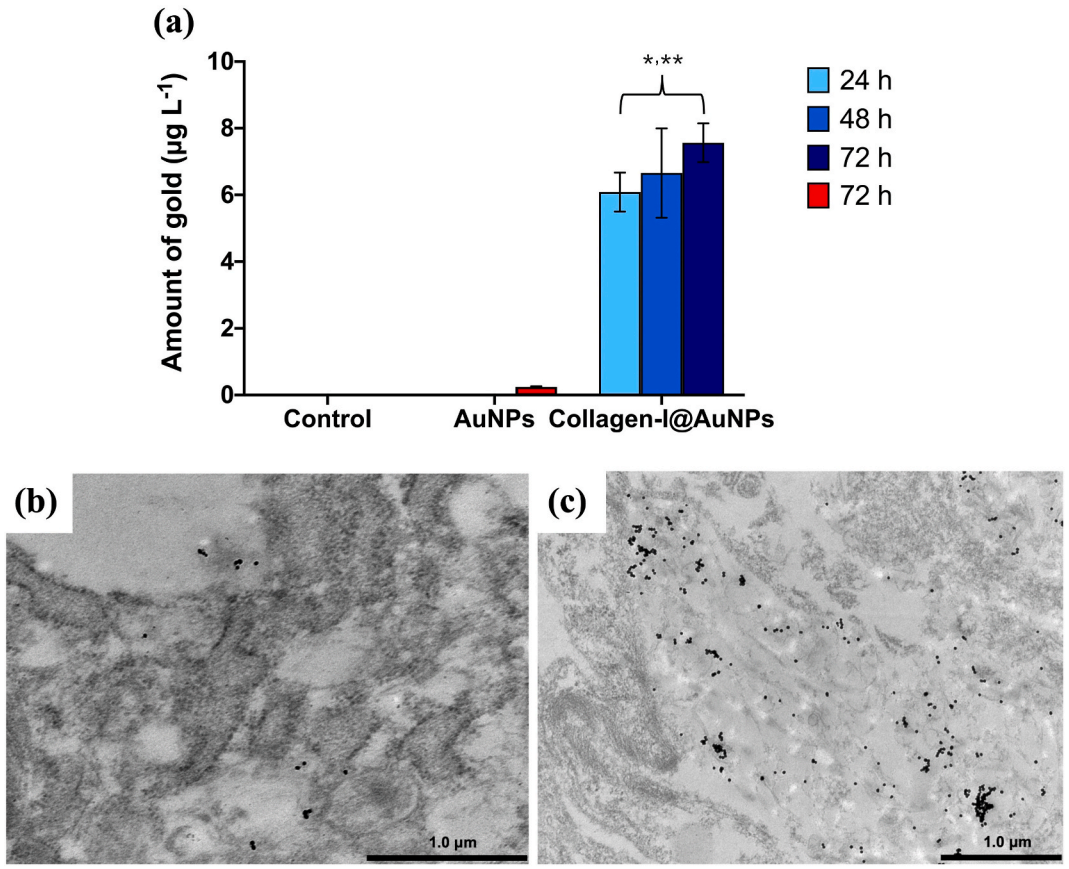

Fig. 5. (a) The gold content detected in scratched HSF cells using the ICP-MS. Untreated cells were used as control cells. *Significant difference in gold content ($P < 0.05$) compared with control (untreated HSF cells) and ** compared with scratched HSF cells treated with AuNPs for 72 h. Statistical analysis was performed using Turkey-Kramer ($n \geq 3$). TEM images of scratched HSF cells treated with (b) AuNPs and (c) Collagen-I@AuNPs for 72 h. (For interpretation of the references to colour in this figure legend, the reader is referred to the Web version of this article.)

efficient internalization of Collagen-I@AuNPs in HSF cells.

TEM images also confirmed the internalization of the particles after culturing scratched HSF cells with AuNPs and Collagen-I@AuNPs for 72 h. As shown in Fig. 5b&c, more particles were present in the scratched cells that were treated with Collagen-I@AuNPs compared to those treated with AuNPs. Collagen-I has been shown to bind to the plasma membrane of fibroblast cells, as reported in Ref. [46]. Consequently, the greater the binding of Collagen-I@AuNPs, the more particles were detected in the scratched HSF cells through endocytosis. Collagen-I is commonly recognized as a fibril-forming collagen [47]. It is widely recognized that collagen is a major component in cellular matrix. Research conducted by Shi et al. [48] demonstrated that Collagen-I present on nanoparticle surface could interact with fibroblasts. An interaction between Collagen-I and HSF cells could occur through and integrin-mediated mechanism [49], which later resulted in the internalization of Collagen-I@AuNPs into the cells. A previous study compared the cellular uptake and toxicity of AuNPs coated with collagen and synthetic polymers. The results indicated that AuNPs coated with collagen were more highly internalized by cells than those coated with synthetic polymer [44]. Our study revealed that collagen-I on the surface of AuNPs significantly improves the uptake dynamics of Collagen-I@AuNPs. A unique characteristic of

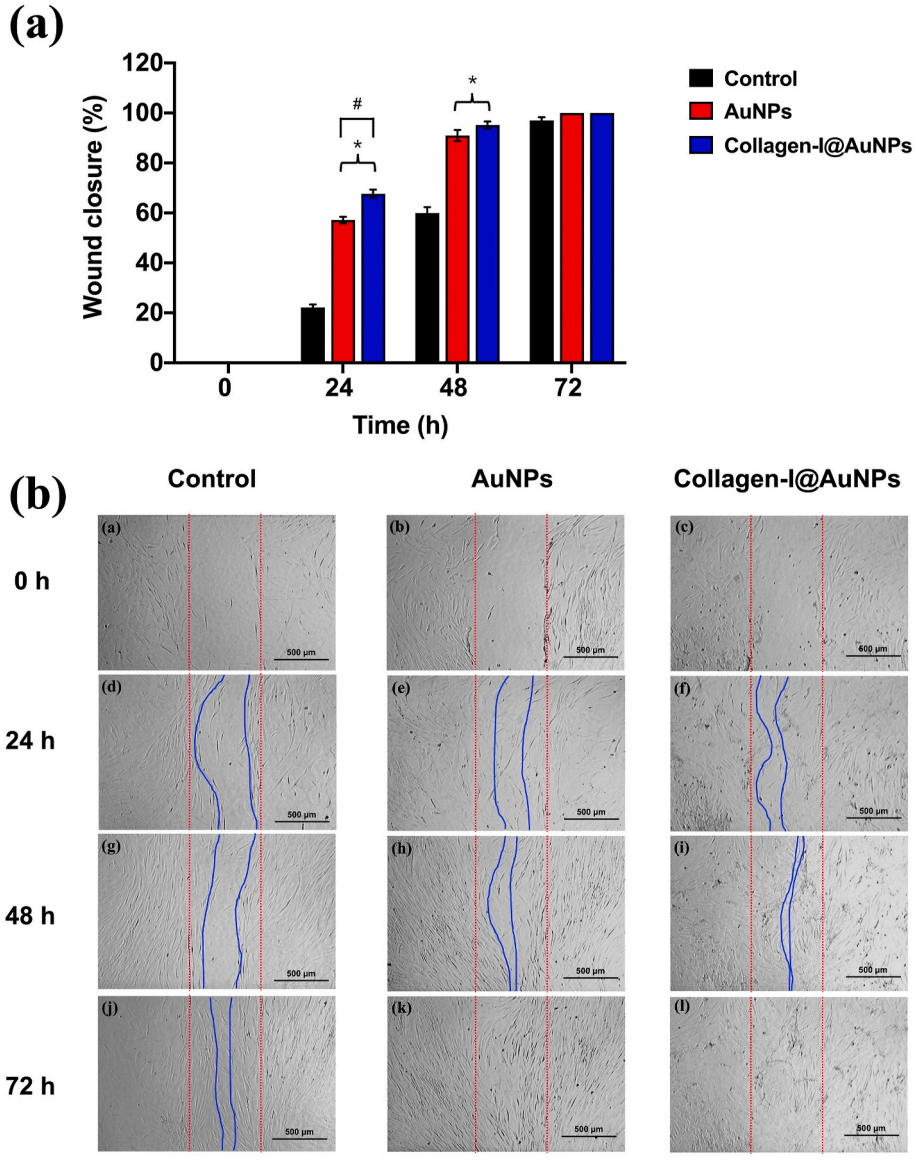

Fig. 6. (a) Percentages of wound closure of scratched HSF cells treated with 3 μg mL^{-1} AuNPs and Collagen-I@AuNPs for 24, 48, and 72 h *Significant difference in wound closure percentage at $P < 0.05$ compared with control cells (untreated HSF cells) at 24 h and at 48 h # Significant difference in wound closure percentage of HSF cells treated with AuNPs and Collagen-I@AuNPs for 24 h at $P < 0.05$. Statistical analysis was performed using the Turkey-Kramer test ($n \geq 11$). (b) Cell migration images of scratched HSF cells treated with 3 μg mL^{-1} AuNPs and Collagen-I@AuNPs for 24 h, 48 h, and 72 h.

collagen is that it is resistant to degradation by several common proteinases, including trypsin, chymotrypsin, and pepsin. However, it can be broken down by collagenases, which are metalloproteinases [50]. In this research, we examined the influence of Collagen-I@AuNPs on the healing of scratched HSF cells *in vitro*. Nevertheless, the extent of biodegradation of collagen-I@AuNPs by collagenases must be considered, particularly *in vivo* environments.

3.4. Effect of AuNPs and Collagen-I@AuNPs on wound closure

The effects of AuNPs and Collagen-I@AuNPs on wound healing *in vitro* were investigated using a wound scratch assay. The monolayer of scratched HSF cells was treated with AuNPs or Collagen-I@AuNPs in medium containing 5 % FBS. Based on our results for cell viability and proliferation, we decided to use only 3 μg mL^{-1} AuNPs and Collagen-I@AuNPs in the wound closure study. This is because this concentration provided good outcomes for cell viability and proliferation. Cellular uptake also confirmed the internalization of particles into HSF cells. As shown in Fig. 6a, scratched HSF cells treated with AuNPs and Collagen-I@AuNPs had a higher wound closure percentage than the untreated cells (control cells). The percentages of wound closure ~57.16 ± 1.31 % and ~67.67 ± 1.67 % were found in scratched HSF cells treated with AuNPs and Collagen-I@AuNPs for 24 h, respectively. These percentages were significantly different from those of untreated cells, which had a wound closure of 22.12 ± 1.22 %. After 48 h of treatment, the percentage of wound closure in scratched HSF cells treated with AuNPs (91.01 ± 2.71 %) and Collagen-I@AuNPs (95.19 ± 1.67 %) increased compared to that at 24 h. The percentage of wound closure in untreated cells increased to 59.96 ± 2.66 %. Complete closure was observed in the scratched HSF cells treated with AuNPs or Collagen-I@AuNPs for 72 h. In untreated scratched HSF cells, the percentage of wound closure was 97.06 ± 1.22 % after culturing for 72 h. These results clearly showed that AuNPs and Collagen-I@AuNPs enhanced the healing process. After 24 h of treatment, Collagen-I@AuNPs (67.67 ± 1.67 % wound closure) accelerated the healing process of scratched HSF cells compared to AuNPs (57.16 ± 1.31 % wound closure). This indicated that Collagen-I plays a vital role in enhancing wound closure. Previous research has reported the influence of Collagen-I on stimulating wound healing [51]. This type of collagen plays a vital role in guiding cell adhesion and migration. The impact of Collagen-I on the induction of F-actin spreading and fibroblast proliferation was demonstrated by Ramadass et al. [52]. Compared to untreated scratched HSF cells, the wound closure percentage of scratched HSF cells treated with AuNPs was also enhanced. This enhancement may be attributed to the antioxidative effects of AuNPs, which could play a vital role in cell migration and wound healing [53]. The cell migration images are shown in Fig. 6b.

3.5. Inflammatory cytokine response and angiogenesis growth factor production by HSF cells after treating with AuNPs and Collagen-I@AuNPs on wound closure

It is well known that pro-inflammatory cytokines (IL-6 and TNF-α) play key roles in the wound healing. IL-6 is a pleiotropic cytokine secreted by fibroblasts and other cell types after exposure to various stimuli or inflammation [54]. The effects of AuNPs and Collagen-I@AuNPs on IL-6 production in the scratched HSF cells were investigated. As seen in Fig. 7a, significant decreases in IL-6 levels were detected in all treated scratched HSF cells and untreated scratched HSF at 48 and 72 h post-wounding compared to 24 h post-wounding in untreated scratched HSF cells. A similar trend of IL-6 decrease at a longer time post-wounding was reported by Wang et al. [55]. A significantly lower IL-6 level in scratched HSF cells treated with AuNPs (45 ± 4.31 pg mL^{-1}) or Collagen-I@AuNPs (39 ± 5.44 pg mL^{-1}) than in untreated cells (79 ± 5.93 pg mL^{-1}) was detected at 48 h post-wounding. A decrease in IL-6 production

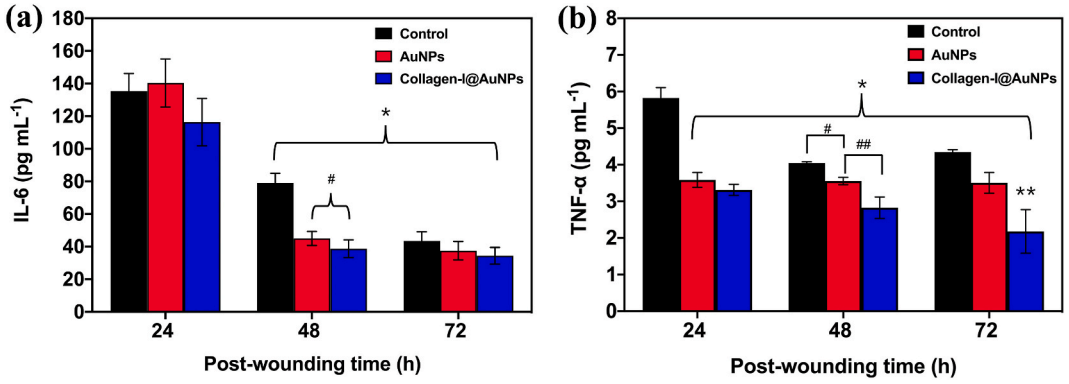

Fig. 7. (a) IL-6 and (b) TNF-α levels of scratched HSF cells treated with 3 μg mL^{-1} AuNPs and Collagen-I@AuNPs for 24, 48, and 72 h *Significant difference at $P < 0.05$ compared with control cells (untreated scratched HSF cells at 24 h). $^{\#(a)}$ Significant difference in IL-6 levels of scratched HSF cells at $P < 0.05$ compared with control cells (untreated scratched HSF cells at 48 h). $^{\#(b)}$ Significant difference in TNF-α levels between untreated scratched HSF cells and scratched HSF cells treated with 3 μg mL^{-1} AuNPs at $P < 0.05$. $^{\#\#}$ Significant difference in TNF-α levels between scratched HSF cells treated with 3 μg mL^{-1} AuNPs and Collagen-I@AuNPs at $P < 0.05$. ** Significant difference in TNF-α levels of scratched HSF cells at $P < 0.05$ compared with control cells (untreated scratched HSF cells) at 72 h post-wounding. Statistical analysis was performed using the Turkey-Kramer test ($n \geq 3$).

was also observed in scratched HSF cells treated with AuNPs (37 ± 5.65 pg mL^{-1}), Collagen-I@AuNPs (34 ± 5.12 pg mL^{-1}), and untreated HSF cells (43 ± 5.71 pg mL^{-1}) at 72 h post-wounding. The lowest concentration of IL-6 was also found in scratched HSF cells treated with Collagen-I@AuNPs (116 ± 14.52 pg mL^{-1}) at 24 h post-wounding. Our results demonstrated that HSF cells that were scratched and treated with Collagen-I@AuNPs exhibited the lowest levels of IL-6 at all three time points of post-wounding.

Similar to IL-6 production, TNF-α levels decreased when there was an increase in the percentage of wound closure (Fig. 7b). The concentrations of TNF-α detected in scratched HSF cells treated with AuNPs and Collagen-I@AuNPs at 24 h post-wounding were 3.59 ± 0.21 and 3.32 ± 0.15 pg mL^{-1}, respectively. These amounts of TNF- α significantly decreased when compared to scratched HSF cells without treatment (5.83 ± 0.28 pg mL^{-1}). At 48 h post-wounding, the TNF-α levels of scratched HSF cells treated with AuNPs and Collagen-I@AuNPs decreased to 3.56 ± 0.10 and 2.83 ± 0.29 pg mL^{-1}, respectively. Significant differences in TNF-α levels were detected between scratched HSF cells treated with Collagen-I@AuNPs and untreated scratched HSF cells. A significant difference was also observed between scratched HSF cells treated with AuNPs and Collagen-I@AuNPs. TNF-α levels of scratched HSF cells treated with AuNPs and Collagen-I@AuNPs at 72 h post-wounding were 3.51 ± 0.28 and 2.18 ± 0.59 pg mL^{-1}, respectively. TNF- α concentrations of untreated scratched HSF cells at 24, 48, and 72 h post-wounding were 5.83 ± 0.28, 4.04 ± 0.04, and 4.35 ± 0.06 pg mL^{-1}, respectively. Scratched HSF cells treated with Collagen-I@AuNPs also had the lowest TNF- α concentrations at all post-wounding periods. It was reported that the levels of IL-6 and TNF-α decreased as the proliferation and migration of fibroblast cells increased during the healing process [55–57]. Our results also demonstrated a decline in the levels of pro-inflammatory cytokines (IL-6 and TNF-α) as HSF cell migration increased. Both cytokines were found at their lowest concentrations in scratched HSF cells treated with Collagen-I@AuNPs. This indicates that the Collagen-I coating on the surface of AuNPs was implicated in wound healing simulation. As reported previously, Collagen-I can increase the synthesis of the extracellular matrix and enhance cell proliferation, resulting in enhancement of the healing process [58,59].

In addition to inflammatory cytokines, growth factors are involved in wound healing. bFGF, in particular, regulates the replication and migration of fibroblast cells [60,61]. As shown in Fig. 8a, our results showed that after scratched HSF cells were treated with 3 μg mL^{-1} AuNPs or Collagen-I@AuNPs for 48 h, the bFGF levels were induced to be higher (45.67 ± 1.40 pg mL^{-1} for AuNPs and 45.20 ± 2.54 pg mL^{-1} for Collagen-I@AuNPs) than untreated scratched HSF cells (38.70 ± 2.54 pg mL^{-1}). At 72 h, the level of bFGF in scratched HSF cells treated with 3 μg mL^{-1} AuNPs decreased from 45.67 ± 1.40 (at 48 h post-wounding) to 43.23 ± 0.76 pg mL^{-1}. A significant increase was observed in scratched HSF cells treated with 3 μg mL^{-1} Collagen-I@AuNPs (52.11 ± 2.34 pg mL^{-1}) compared to untreated scratched HSF cells (41.09 ± 1.43 pg mL^{-1}). A significant difference in bFGF levels between scratched HSF cells treated with AuNPs and Collagen-I@AuNPs was also observed at 72 h post-wounding. This indicated that Collagen-I on the surface of AuNPs affected bFGF production. Collagen in wound dressing has been reported to enhance wound healing by stimulating fibroblast movement [62].

Another growth factor investigated in this study was VEGF. VEGF is released by various cells, including fibroblasts, and plays a vital role in wound healing [63]. VEGF is involved in angiogenesis, which is important in the proliferative phase of wound healing [64]. VEGF has been found to promote the migration and collagen production of skin fibroblast [65]. A significant induction of VEGF levels was detected in scratched HSF cells treated with 3 μg mL^{-1} AuNPs or Collagen-I@AuNPs at 24, 48, and 72 h post-wounding when compared to untreated scratched HSF cells (Fig. 8b). Significant induction of VEGF between AuNPs and Collagen-I@AuNPs was observed at 72 h post-wounding. The concentrations of VEGF were 34.00 ± 1.22 pg mL^{-1} (AuNPs) and 45.00 ± 2.63 pg mL^{-1}(Collagen-I@AuNPs).

AuNPs could also induce VEGF levels; however, it clearly showed that Collagen-I@AuNPs enhanced the production of bFGF and VEGF more than AuNPs alone. This could be the fact that Collagen-I@AuNPs were taken up more readily by HSF cells (as shown in

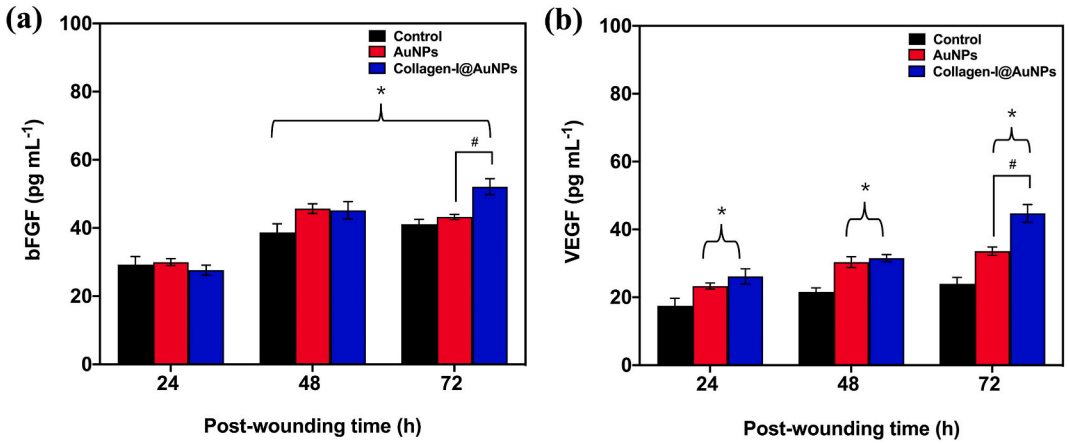

Fig. 8. (a) bFGF and (b) VEGF levels of scratched HSF cells treated with 3 μg mL^{-1} AuNPs and Collagen-I@AuNPs for 24, 48, and 72 h. *Significant difference in bFGF and VEGF levels of scratched HSF cells at $P < 0.05$ compared with control cells (untreated scratched HSF cells at 24 h (for a) and at all post-wounding times (for b)). #Significant difference in bFGF and VEGF levels between scratched HSF cells treated with 3 μg mL^{-1} AuNPs and Collagen-I@AuNPs at $P < 0.05$. Statistical analysis was performed using the Turkey-Kramer test ($n \geq 3$).

Fig. 5), leading to an increase in the levels of bFGF and VEGF. The enhancement of these growth factors can contribute to cell migration.

Our research focused on examining the effect of Collagen-I@AuNPs on pro-inflammatory cytokine production, specifically IL-6 and TNF-α, as well as on growth factor (bFGF and VEGF) production. As previously discussed, these molecules play crucial roles in wound healing. Although we did not delve into the effect of Collagen-I@AuNPs on other factors that contribute to wound healing, we acknowledged that numerous additional factors are involved in this process. For example, a comprehensive review article by Diller and Tabor [66] reported that ECM can enhance cellular activities, such as cell adherence, cellular signaling, and tissue anchoring. Fibroblasts are responsible for the remodeling of the ECM by secreting matrix metalloproteinases (MMPs) and other ECM components. It has been reported that the interaction between fibroblasts and the ECM can be considered as a form of autocrine regulation, which is essential for wound healing [67]. A potential area of interest for future investigation is the examination of how Collagen-I@AuNPs affect the association between skin fibroblasts and ECM. However, our findings showed that Collagen-I@AuNPs promoted HSF cell migration. This implies that Collagen-I@AuNPs may not have a negative impact on the fibroblast-ECM connection. Chemokines, particularly interleukin-8 (IL-8), also play vital roles in cell migration and proliferation. However, elevation of IL-8 was reported to delay wound healing by inhibiting fibroblast-populated collagen lattice contraction [68]. Future studies should investigate the effects of Collagen-I@AuNPs on IL-8 secretion.

It has been reported that the migration and proliferation of cells are influenced by fibroblast growth factors (FGFs) through various mechanisms involving the activation of different pathways. The migratory pathway is facilitated by the Src family of protein tyrosine kinases (SRC) and p38 mitogen-activated protein kinase (MAPK) signaling pathways. The activation of ERK (extracellular signal-regulated kinase) is crucial in promoting cell proliferation [69]. According to our findings, there was a significant increase in bFGF production in HSF cells treated with Collagen-I@AuNPs (as shown in Fig. 8a). It is worth noting that Mendieta et al. [70] reported that the RAS/RAF/MEK/ERK (MAPK) signaling pathway is regulated by bFGF. This suggests that Collagen-I@AuNPs may play a role in the activation of these pathways. Additionally, as illustrated in Fig. 8b–a significant increase in VEGF levels was detected. Kasowanjete et al. [71] reported that VEGF is associated with intracellular signaling pathways, including PI3K/AKT/mTOR, which play a role in regulating cell growth, metabolism, proliferation, apoptosis, and protein synthesis. The enhancement of VEGF expression in HSF cells treated with Collagen-I@AuNPs may be linked to the activation of PI3K/AKT/mTOR. Overall, the findings from our study suggested that Collagen-I@AuNPs appear to have an impact on the signaling pathways that are involved in the healing of wounds. More research is needed to examine the effect of Collagen-I@AuNPs on these signaling pathways in the future.

4. Conclusions

In this study Collagen-I was associated with AuNPs to form Collagen-I@AuNPs. Collagen-I@AuNPs were not toxic to the HSF cells used in this study. Furthermore, they enhanced cell proliferation and migration resulting in rapid wound healing. In addition, Collagen-I@AuNPs reduced the levels of inflammatory cytokines (IL-6 and TNF-α), while increasing the production of vital growth factors (bFGF and VEGF), which play a major role in healing process. The results suggest that Collagen-I is a suitable candidate for association with AuNPs. Collagen-I stabilized on the surface of AuNPs could enhance the cellular uptake of particles by HSF cells compared to that of AuNPs. The high degree of internalization of Collagen-I@AuNPs could be a key mechanism that lead to a high healing potential for skin cell injuries. Therefore, Collagen-I@AuNPs can serve as potent particles for treating skin injuries. A more detailed study *in vivo* should be conducted to explore their potential more thoroughly.

CRediT authorship contribution statement

Sasiprapa Poomrattanangoon: Writing – original draft, Visualization, Validation, Formal analysis. **Dakrong Pissuwan:** Writing – review & editing, Visualization, Validation, Supervision, Funding acquisition, Conceptualization.

Declaration of competing interest

The authors declare that they have no known competing financial interests or personal relationships that could have appeared to influence the work reported in this paper.

Acknowledgments

This work was mainly funded by Mahidol University (Fundamental Fund: Fiscal Year 2023 by National Science and Innovation Fund (NSRF), Thailand, grant no. FF-077/2566) to D. P. Funding support from the Royal Golden Jubilee Ph.D. Program, Thailand (PHD/0195/2560) under the National Research Council of Thailand (NRCT), Thailand to S. P. for her Ph.D. study and partial research support. The authors thank the Center of Excellence on Environmental Health and Toxicology (EHT) and Center for Scientific Instrumentation and Platform Services, Faculty of Science, Mahidol University.

Appendix ASupplementary data

Supplementary data to this article can be found online at https://doi.org/10.1016/j.heliyon.2024.e33302.

References

[1] M. Stojko, D. Wolny, J. Włodarczyk, Nonwoven releasing Propolis as a potential new wound healing method—a review, Molecules 26 (2021) 5701.
[2] A. Oliveira, S. Simoes, A. Ascenso, C.P. Reis, Therapeutic advances in wound healing, J. Dermatol. Treat. 33 (2022) 2–22.
[3] R. Edwards, K.G. Harding, Bacteria and wound healing, Curr. Opin. Infect. Dis. 17 (2004) 91–96.
[4] S.K. Nethi, S. Das, C.R. Patra, S. Mukherjee, Recent advances in inorganic nanomaterials for wound-healing applications, Biomater. Sci. 7 (2019) 2652–2674.
[5] J.K. Stechmiller, Understanding the role of nutrition and wound healing, Nutr. Clin. Pract. 25 (2010) 61–68.
[6] E. Arribas-López, N. Zand, O. Ojo, M.J. Snowden, T. Kochhar, The effect of amino acids on wound healing: a systematic review and meta-analysis on arginine and glutamine, Nutrients 13 (2021) 2498.
[7] S.-W. Chang, M.J. Buehler, Molecular biomechanics of collagen molecules, Mater. Today 17 (2014) 70–76.
[8] S.S. Mathew-Steiner, S. Roy, C.K. Sen, Collagen in wound healing, Bioengineering 8 (2021) 63.
[9] M. Xue, C.J. Jackson, Extracellular matrix reorganization during wound healing and its impact on abnormal scarring, Adv. Wound Care 4 (2015) 119–136.
[10] E. Davison-Kotler, W.S. Marshall, E. García-Gareta, Sources of collagen for biomaterials in skin wound healing, Bioengineering 6 (2019) 56.
[11] A. Rangaraj, K. Harding, D. Leaper, Role of collagen in wound management, Wounds U. K. 7 (2011) 54–63.
[12] R.J. Kadhim, E.H. Karsh, Z.J. Taqi, M.S. Jabir, Biocompatibility of gold nanoparticles: in-vitro and In-vivo study, Mater. Today: Proc. 42 (2021) 3041–3045.
[13] V. Pivodová, J. Franková, A. Galandáková, J. Ulrichová, In vitro AuNPs' cytotoxicity and their effect on wound healing, Nanobiomedicine 2 (2015) 7.
[14] D. Pissuwan, T. Niidome, Polyelectrolyte-coated gold nanorods and their biomedical applications, Nanoscale 7 (2015) 59–65.
[15] D. Pissuwan, S.M. Valenzuela, M.B. Cortie, Therapeutic possibilities of plasmonically heated gold nanoparticles, Trends Biotechnol. 24 (2006) 62–67.
[16] D. Pissuwan, T. Niidome, M.B. Cortie, The forthcoming applications of gold nanoparticles in drug and gene delivery systems, J. Contr. Release 149 (2011) 65–71.
[17] S. Chotithammakul, M.B. Cortie, D. Pissuwan, Comparison of single-and mixed-sized gold nanoparticles on lateral flow assay for albumin detection, Biosensors 11 (2021) 209.
[18] D. Pissuwan, C. Gazzana, S. Mongkolsuk, M.B. Cortie, Single and multiple detections of foodborne pathogens by gold nanoparticle assays, Wiley Interdiscip. Rev. Nanomed. Nanobiotechnol. 12 (2020) e1584.
[19] D. Pissuwan, S. Poomrattanangoon, P. Chungchaiyart, Trends in using gold nanoparticles for inducing cell differentiation: a review, ACS Appl. Nano Mater. 5 (2022) 3110–3120.
[20] S.-A. Chen, H.-M. Chen, Y.-D. Yao, C.-F. Hung, C.-S. Tu, Y.-J. Liang, Topical treatment with anti-oxidants and Au nanoparticles promote healing of diabetic wound through receptor for advance glycation end-products, Eur. J. Pharmaceut. Sci. 47 (2012) 875–883.
[21] Z. Batool, G. Muhammad, M.M. Iqbal, M.S. Aslam, M.A. Raza, N. Sajjad, M. Abdullah, N. Akhtar, A. Syed, A.M. Elgorban, Hydrogel assisted synthesis of gold nanoparticles with enhanced microbicidal and in vivo wound healing potential, Sci. Rep. 12 (2022) 6575.
[22] J. Toczek, M. Sadłocha, K. Major, R. Stojko, Benefit of silver and gold nanoparticles in wound healing process after endometrial cancer protocol, Biomedicines 10 (2022) 679.
[23] S. Barathmanikanth, K. Kalishwaralal, M. Sriram, S.R.K. Pandian, H.-s. Youn, S. Eom, et al., Anti-oxidant effect of gold nanoparticles restrains hyperglycemic conditions in diabetic mice, J. Nanobiotechnol. 8 (2010) 16.
[24] R.S. Darweesh, N.M. Ayoub, S. Nazzal, Gold nanoparticles and angiogenesis: molecular mechanisms and biomedical applications, Int. J. Nanomed. 14 (2019) 7643–7653.
[25] C. Roma-Rodrigues, A. Heuer-Jungemann, A.R. Fernandes, A.G. Kanaras, P.V. Baptista, Peptide-coated gold nanoparticles for modulation of angiogenesis *in vivo*, Int. J. Nanomed. (2016) 2633–2639.
[26] M.G. Tonnesen, X. Feng, R.A. Clark, Angiogenesis in wound healing, J. Invest. Dermatol. Symp. Proc. 5 (2000) 40–46.
[27] S. Li, Q. Tang, H. Xu, Q. Huang, Z. Wen, Y. Liu, C. Peng, Improved stability of KGF by conjugation with gold nanoparticles for diabetic wound therapy, Nanomed 14 (2019) 2909–2923.
[28] O. Akturk, K. Kismet, A. C Yasti, S. Kuru, M.E. Duymus, F. Kaya, et al., Collagen/gold nanoparticle nanocomposites: a potential skin wound healing biomaterial, J. Biomater. Appl. 31 (2016) 283–301.
[29] L. Castaneda, J. Valle, N. Yang, S. Pluskat, K. Slowinska, Collagen cross-Linking with Au nanoparticles, Biomacromolecules 9 (2008) 3383–3388.
[30] R. Xing, T. Jiao, L. Yan, G. Ma, L. Liu, L. Dai, et al., Colloidal gold–collagen protein core–shell nanoconjugate: one-step biomimetic synthesis, Layer-bylayer assembled film, and controlled cell growth, ACS Appl. Mater. Interfaces 7 (2015) 24733–24740.
[31] J. Kimling, M. Maier, B. Okenve, V. Kotaidis, H. Ballot, A. Plech, Turkevich method for gold nanoparticle synthesis revisited, J. Phys. Chem. B 110 (2006) 15700–15707.
[32] M. Iqbal, G. Usanase, K. Oulmi, F. Aberkane, T. Bendaikha, H. Fessi, et al., Preparation of gold nanoparticles and determination of their particles size via different methods, Mater. Res. Bull. 79 (2016) 97–104.
[33] C. Kim, S.S. Agasti, Z. Zhu, L. Isaacs, V.M. Rotello, Recognition-mediated activation of therapeutic gold nanoparticles inside living cells, Nat. Chem. 2 (2010) 962–966.
[34] V.S. Cardoso, M. de Carvalho Filgueiras, Y.M. Dutra, R.H.G. Teles, A.R. de Araújo, F.L. Primo, et al., Collagen-based silver nanoparticles: study on cell viability, skin permeation, and swelling inhibition, Mater. Sci. Eng. C 74 (2017) 382–388.
[35] G.I. Sakellari, N. Hondow, P.H.E. Gardiner, Factors influencing the surface Functionalization of citrate stabilized gold nanoparticles with cysteamine, 3-mer-captopropionic acid or l-selenocystine for aensor applications, Chemisensors 8 (2020) 80.
[36] B.B. Doyle, E. Bendit, E.R. Blout, Infrared spectroscopy of collagen and collagen-like polypeptides, Biopolymers 14 (1975) 937–957.
[37] Y. Abe, S. Krimm, Normal vibrations of crystalline polyglycine I, Biopolymers 11 (1972) 1817–1839.
[38] K.J. Payne, A. Veis, Fourier transform IR spectroscopy of collagen and gelatin solutions: Deconvolution of the amide I band for conformational studies, Biopolymers 27 (1988) 1749–1760.
[39] S. Krimm, J. Bandekar, Vibrational spectroscopy and conformation of peptides, polypeptides, and proteins, Adv. Protein Chem. 38 (1986) 181–364.
[40] J. Muyonga, C. Cole, K. Duodu, Characterisation of acid soluble collagen from skins of young and adult Nile perch (Lates niloticus), Food Chem. 85 (2004) 81–89.
[41] D.D. Rajaratanam, H. Ariffin, M.A. Hassan, N.M.A. Nik Abd Rahman, H. Nishida, *In vitro* cytotoxicity of superheated steam hydrolyzed oligo ((R)-3-hydroxybutyrate-co-(R)-3-hydroxyhexanoate) and characteristics of its blend with poly (L-lactic acid) for biomaterial applications, PLoS One 13 (2018) e0199742.
[42] D.M. Reilly, J. Lozano, Skin collagen through the lifestages: Importance for skin health and beauty, Plast. Aesthet. Res. 8 (2021) 2.
[43] P. Wang, Q. Wu, F. Wang, Y. Zhang, L. Tong, T. Jiang, C. Gu, S. Huang, H. Wang, S. Bu, Evaluating cellular uptake of gold nanoparticles in HL-7702 and HepG2 cells for plasmonic photothermal therapy, Nanomed 13 (2018) 2245–2259.
[44] O.T. Marisca, K. Kantner, C. Pfeiffer, Q. Zhang, B. Pelaz, N. Leopold, W.J. Parak, J. Rejman, Comparison of the *in vitro* uptake and toxicity of collagen-and synthetic polymer-coated gold nanoparticles, Nanomaterials 5 (2015) 1418–1430.
[45] L. Zhang, D. Wang, H. Yu, Fabrication of protein-coated titanium dioxide nanoparticles for cellular uptake fluorescence imaging and treatment of colorectal cancer, Mater. Res. Express 8 (2021) 125008.
[46] B. Goldberg, Binding of soluble Collagen-I molecules to the fibroblast plasma membrane, Cell 16 (1979) 265–275.
[47] K. Gelse, E. Pöschl, T. Aigner, Collagens—structure, function, and biosynthesis, Adv. Drug Deliv. Rev. 55 (2003) 1531–1546.
[48] Y. Shi, C. Hélary, T. Coradin, Exploring the Cell–Protein–Mineral Interfaces: Interplay of Silica (Nano)rods@collagen Biocomposites with Human Dermal Fibroblasts vol. 1, Materials Today Bio, 2019 100004.
[49] D. Dutta, J. Markhoff, N. Suter, K. Rezwan, D. Brüggemann, Effect of collagen nanofibers and silanization on the interaction of HaCaTkeratinocytes and 3T3 fibroblasts with alumina nanopores, ACS Appl. Bio Mater. 4 (2021) 1852–1862.

[50] M.F. Paige, A.C. Lin, M.C. Goh, Real-time enzymatic biodegradation of collagen fibrils monitored by atomic force microscopy, Int. Biodeterior. Biodegrad. 50 (2002) 1–10.
[51] P.E. Shamhart, J.E. Naugle, E.R. Olson, M.A. Hruska, K.J. Doane, J.G. Meszaros, Cardiac fibroblast migration during *in vitro* wound healing: the role of specific collagen substrates, FASEB 21 (2007) A1428–A1429.
[52] S.K. Ramadass, L.S. Nazir, R. Thangam, R.K. Perumal, I. Manjubala, B. Madhan, et al., Type I collagen peptides and nitric oxide releasing electrospun silk fibroin scaffold: a multifunctional approach for the treatment of ischemic chronic wounds, Colloids Surf. B Biointerfaces 175 (2019) 636–643.
[53] J.-G. Leu, S.-A. Chen, H.-M. Chen, W.-M. Wu, C.-F. Hung, Y.-D. Yao, C.-S. Tu, Y.-J. Liang, The effects of gold nanoparticles in wound healing with antioxidant epigallocatechin gallate and α-lipoic acid, Nanomed. Nanotechnol. Biol. Med. 8 (2012) 767–775.
[54] M.R. Duncan, B. Berman, Stimulation of collagen and glycosaminoglycan production in cultured human adult dermal fibroblasts by recombinant human interleukin 6, J. Invest. Dermatol. 97 (1991) 686–692.
[55] Y. Wang, Y. Feng, J. Yan, X. Han, P. Song, Y. Wu, X. Wang, Z. Mu, X. Li, H. Zhang, Spiky surface topography of heterostructured nanoparticles for programmable acceleration of multistage wound healing, Mater. Today Nano 23 (2023) 100351.
[56] J. Tian, K.K. Wong, C.M. Ho, C.N. Lok, W.Y. Yu, C.M. Che, J.F. Chiu, P.K. Tam, Topical delivery of silver nanoparticles promotes wound healing, ChemMedChem 2 (2007) 129–136.
[57] S. Mo, P.-S. Chung, J.C. Ahn, 630 nm-OLED accelerates wound healing in mice via regulation of cytokine release and genes expression of growth factors, Curr. Opt. Photonics 3 (2019) 485–495.
[58] E.J. Orwin, A. Hubel, In vitro culture characteristics of corneal epithelial, endothelial, and keratocyte cells in a native collagen matrix, Tissue Eng. 6 (2000) 307–319.
[59] R. Sklenářová, N. Akla, M.J. Latorre, J. Ulrichová, J. Franková, Collagen as a biomaterial for skin and corneal wound healing, J. Funct. Biomater. 13 (2022) 249.
[60] D.B. Hom, G.M. Unger, K.J. Pernell, J.C. Manivel, Improving surgical wound healing with basic fibroblast growth factor after radiation, Laryngoscope 115 (2005) 412–422.
[61] L.L. Root, G.D. Shipley, Human dermal fibroblasts express multiple bFGF and aFGF proteins, In Vitro Cell. Dev. Biol. Anim. 27 (1991) 815–822.
[62] S. Gajbhiye, S. Wairkar, Collagen fabricated delivery systems for wound healing: a new roadmap, Biomater. Adv. 142 (2022) 213152.
[63] R. Savari, M. Shafiei, H. Galehdari, M. Kesmati, Expression of VEGF and TGF-β genes in skin wound healing process induced using phenytoin in male rats, Jundishapur J. Health Sci. 11 (2019) e86041.
[64] K.E. Johnson, T.A. Wilgus, Vascular endothelial growth factor and angiogenesis in the regulation of cutaneous wound repair, Adv. Wound Care 3 (2014) 647–661.
[65] C.-C. Chung, Y.-K. Lin, Y.-C. Chen, Y.-H. Kao, T.-I. Lee, Y.-J. Chen, Vascular Endothelial Growth Factor Enhances Profibrotic Activities through Modulation of Calcium Homeostasis in Human Atrial Fibroblasts, 100, Laboratory Investigation, 2020, pp. 285–296.
[66] R.B. Diller, A.J. Tabor, The role of the extracellular matrix (ECM) in wound healing: a review, Biomimetics 7 (2022) 87.
[67] L.E. Tracy, R.A. Minasian, E.J. Caterson, Extracellular matrix and dermal fibroblast function in the healing wound, Adv. Wound Care 5 (2016) 119–136.
[68] J.A. Iocono, C.R. Kevin, D.G. Remick, B.W. Gillespie, P.H. Ehrlich, W.L. Garner, Interleukin-8 levels and activity in delayed-healing human thermal wounds, Wound Repair Regen. 8 (2000) 216–225.
[69] M. Farooq, A.W. Khan, M.S. Kim, S. Choi, The role of fibroblast growth factor (FGF) signaling in tissue repair and regeneration, Cells 10 (2021) 3242.
[70] P. Viaña-Mendieta, M.L. Sánchez, J. Benavides, Rational selection of bioactive principles for wound healing applications: growth factors and antioxidants, Int. Wound J. 19 (2022) 100–113.
[71] P. Kasowanjete, S.S. Dhilip Kumar, N.N. Houreld, A review of photobiomodulation on PI3K/AKT/mTOR in wound healing, J. Photochem. Photobiol., A 19 (2024) 100215.
[72] J. Kimling, M. Maier, B. Okenve, V. Kotaidis, H. Ballot, A. Plech, Turkevich method for gold nanoparticle synthesis revisited, J. Phys. Chem. B 110 (2006) 15700–15707.
[73] M. Iqbal, G. Usanase, K. Oulmi, F. Aberkane, T. Bendaikha, H. Fessi, N. Zine, G. Agusti, E.-S. Errachid, A. Elaissari, Preparation of gold nanoparticles and determination of their particles size via different methods, Mater. Res. Bull. 79 (2016) 97–104.
[74] C. Kim, S.S. Agasti, Z. Zhu, L. Isaacs, V.M. Rotello, Recognition-mediated activation of therapeutic gold nanoparticles inside living cells, Nat. Chem. 2 (2010) 962–966.
[75] G.I. Sakellari, N. Hondow, P.H. Gardiner, Factors influencing the surface functionalization of citrate stabilized gold nanoparticles with cysteamine, 3-mercaptopropionic acid or l-selenocystine for sensor applications, Chemosensors 8 (2020) 80.
[76] B.B. Doyle, E. Bendit, E.R. Blout, Infrared spectroscopy of collagen and collagen-like polypeptides, Biopolymers 14 (1975) 937–957.